Cytometry Part A 69A:1020–1027 (2006)

High Intensity Solid-State UV Source for Time-Gated Luminescence Microscopy

Russell Connally,* Dayong Jin, and James Piper
Centre for Laser Applications, Division of Information and Communications Science, Department of Physics, Macquarie University, Sydney, Australia

Received 29 August 2005; Revision Received 15 May 2006; Accepted 30 May 2006

Background: The unique discriminative ability of immunofluorescent probes can be severely compromised when probe emission competes against naturally occurring, intrinsically fluorescent substances (autofluorophores). Luminescence microscopes that operate in the time-domain can selectively resolve probes with long fluorescence lifetimes ($\tau > 100$ μs) against short-lived fluorescence to deliver greatly improved signal-to-noise ratio (SNR). A novel time-gated luminescence microscope design is reported that employs an ultraviolet (UV) light emitting diode (LED) to excite fluorescence from a europium chelate immunoconjugate with a long fluorescence lifetime.
Methods: A commercial Zeiss epifluorescence microscope was adapted for TGL operation by fitting with a time-gated image-intensified CCD camera and a high-power (100 mW) UV LED. Capture of the luminescence was delayed for a precise interval following excitation so that autofluorescence was suppressed. *Giardia* cysts were labeled in situ with antibody conjugated to a europium chelate (BHHST) with a fluorescence lifetime >500 μs.
Results: BHHST-labeled *Giardia* cysts emit at 617 nm when excited in the UV and were difficult to locate within the matrix of fluorescent algae using conventional fluorescence microscopy, and the SNR of probe to autofluorescent background was 0.51:1. However in time-gated luminescence mode with a gate-delay of 5 μs, the SNR was improved to 12.8:1, a 25-fold improvement.
Conclusion: In comparison to xenon flashlamps, UV LEDs are inexpensive, easily powered, and extinguish quickly. Furthermore, the spiked emission of the LED enabled removal of spectral filters from the microscope to significantly improve efficiency of fluorescence excitation and capture. © 2006 International Society for Analytical Cytology

Key terms: UV LED; time-gated luminescence; microscopy; lanthanide; *Giardia*

Fluorescence-based techniques provide a powerful means for both the qualitative and quantitative detection of biomolecules. Fluorescence techniques can provide exquisite sensitivity, sufficient for the detection of a single molecule when conditions are optimized (1); however, probes can lose much of their discriminatory power when viewed in the presence of autofluorescence. Organic and inorganic autofluorophores are ubiquitous in nature and some materials fluoresce with great intensity, obscuring or diminishing the visibility of synthetic fluorescent probes (2). Spectral selection techniques (emission and excitation filters) are useful in suppressing autofluorescence but are not always applicable because of the abundance and spectral range of autofluorophores (3). Autofluorescence is typically a short-lived phenomenon with excited-state lifetimes measured in nanoseconds for most common autofluorophores (2,4), and substances differing by less than a nanosecond in fluorescence lifetime can be resolved using time-resolved fluorescence (TRF) techniques. A sinusoidal modulation of the excitation source induces a phase (φ) delayed modulation in fluorescence intensity from which fluorescence lifetime can be determined using φ and modulation frequency parameters (5).

Although it is possible to discriminate probe fluorescence from autofluorescence using a TRF microscope operating in the frequency domain, a simpler and much less costly instrument operating in the time domain can be built if a fluorophore with a long fluorescence lifetime is employed. Lanthanide (Eu^{3+} or Tb^{3+}) chelate fluorescent probes have exceptionally long fluorescence lifetimes reaching milliseconds for some compounds (6–10). The time-gated luminescence microscope (TGLM) described in this report was used in conjunction with the europium chelate fluorophore BHHST ((4,4-bis-(1,1,1,2,2,3,3-heptafluoro-4,6-hexanedion-6-yl) sulfonyl-aminopropyl-ester-*N*-succinimide-ester-*o*-terphenyl)) that has a fluorescence lifetime greater than 600 μs (11). The very large difference in τ between typical autofluorophores and synthetic lanthanide chelates was conveniently exploited using time-gated luminescence (TGL) to eliminate background signal and permit detection electronics to operate

*Correspondence to: Russell Connally.
E-mail: rconnall@ics.mq.edu.au
Published online in Wiley InterScience (www.interscience.wiley.com).
DOI: 10.1002/cyto.a.20326

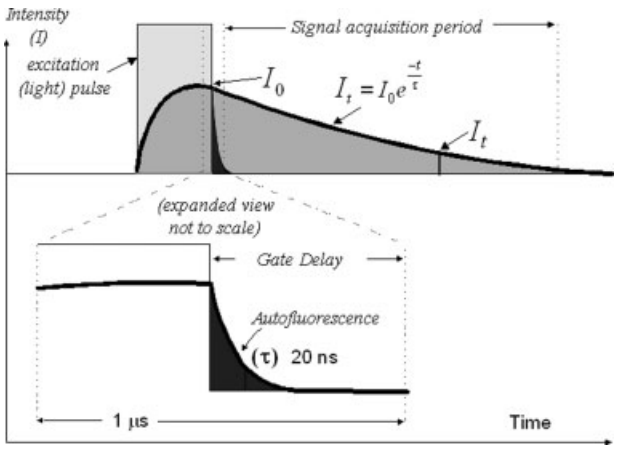

FIG. 1. Time-gated luminescence techniques exploit the large difference in fluorescence lifetime (τ) between common organic autofluorophores (<100 ns) and lanthanide chelates (>300 μs). Once excitation has ceased, there is a rapid decrease in autofluorescence intensity compared to the persistent emission observed from the long-lived fluorescent chelate. The figure shows a single capture cycle and typically the weak time-resolved emission is integrated over hundreds of cycles using a sensitive image-intensified time-gated CCD camera.

at maximum gain. TGL instrumentation designed to capture only long-lived fluorescence emission is technically simple and well suited to suppress autofluorescence.

Time domain techniques (also known as pulse fluorometry) rely on a brief excitation pulse of light to excite fluorescence emission from the sample. The excitation pulse should ideally terminate with a rapid falling edge to ensure that the time-dependent fluorescence emission can be captured free of excitation energy. Figure 1 illustrates both short-lived (nanoseconds) and long-lived fluorescence decay. Certain lanthanide metal chelates have exceptionally long fluorescence lifetimes (11–13), and the large difference in τ enables effective suppression of background, greatly enhancing detection efficiency. Less than 1% of the microorganisms found in the environment respond to culture, and the detection of rare organisms in situ using conventional fluorescence techniques can be exceedingly difficult (14). TGL techniques are particularly advantageous in the detection of rare-events, since the method results in high contrast labeled target against a near void background, greatly increasing the likelihood of detection.

Early luminescence time-gated instruments employed chopper wheels as inexpensive pulsed excitation sources; however, the pulse profile was characterized by a slow rising and falling edge that imposed limits on resolution and sensitivity (15–17). Other limitations of chopper wheels include the inflexible nature of the pulse regime, the inefficient use of light energy, and the risk of image-blur arising from drive motor vibration. Ultraviolet (UV) excitation (300–350 nm) is required for most lanthanide chelate fluorescent probes (18) and nitrogen lasers have found favor as a pulsed excitation source, since they emit short (~3 ns) powerful pulses in the UV (337 nm) and are relatively inexpensive. The low repetition rate of N_2 lasers (10–60 Hz) is a significant detraction and their rapid high-voltage discharge radiates an intense electromagnetic pulse that can cause instrumentation problems. Helium–cadmium (HeCd) lasers are relatively economical continuous wave sources of UV that can be controlled by quartz acousto-optical modulation (AOM) to generate the required short UV pulses for lanthanide chelate TRF studies. Platinum and palladium porphyrin fluorophores have shorter lifetimes ($\tau < 100$ μs) and they can be excited in the blue or violet spectral region, permitting the use of readily available argon-ion lasers (488-nm line) gated with an AOM (19). Gas-discharge lasers require substantial electrical power input and generate significant heat that must be dissipated. Furthermore, the AOM requires a high-voltage RF drive signal and only a small portion of the input laser beam is modulated and available for sample excitation. Gas-discharge laser excitation systems are bulky, expensive, and unreliable when compared with solid-state sources; but until the recent introduction of UV light emitting diodes (LEDs), there were no convenient solid-state alternatives. Engineering samples of a new high-power (100 mW) LED operating at 365 nm were released in late 2004. These devices are fabricated from indium gallium nitride (InGaN) and emit radiation in a narrow band centered at 365 nm with a full-width half maximum (FWHM) range of 10 nm. LEDs are easily driven with low voltages and switch rapidly within nanoseconds; moreover, they offer very high repetition rates to accelerate image acquisition times.

To our knowledge, we are the first to report the existence of low intensity self-excited visible luminescence from GaN-based LEDs that persisted for some time following switch-off and that can present a problem when the devices are used in pulse fluorometry applications. We investigated the suitability of these devices as excitation sources for TGLM and this is the first report of both the temporal and spectral characteristics of excitation pulses obtained from UV LEDs.

MATERIALS AND METHODS

The time-resolved fluorescence microscope (TGLM) used in the present study has been described in detail previously (3,20). In brief, the original TGLM was built using a conventional epifluorescence microscope equipped with a xenon flashlamp excitation source and a time-gated image-intensified CCD camera (DiCam-Pro; PCO Computer Optics, Kelheim, Germany). Integrated with the camera was a 25-mm Hamamatsu microchannel plate image intensifier (12-μm channels) with shutter speeds down to 3 ns. Resolution of the Peltier-cooled CCD element was 1,280 × 1,024 (SVGA) at 12 bits (4,096 counts). The instrument as a whole was controlled by a microprocessor to synchronize the excitation and capture sequence. This microscope was modified for the work reported here by replacing the xenon flashlamp with a high-power UV LED (NCCU033; Nichia Corp., Japan). The LED was obtained from the manufacturer ready-mounted on a square aluminium heatsink (20 × 20 mm) that was subsequently machined to size and fitted in place of the excitation filter within the microscope filter-cube (see Fig. 2). An aspheric lens (C220-TMA, $f = 11$ mm; Thorlabs,

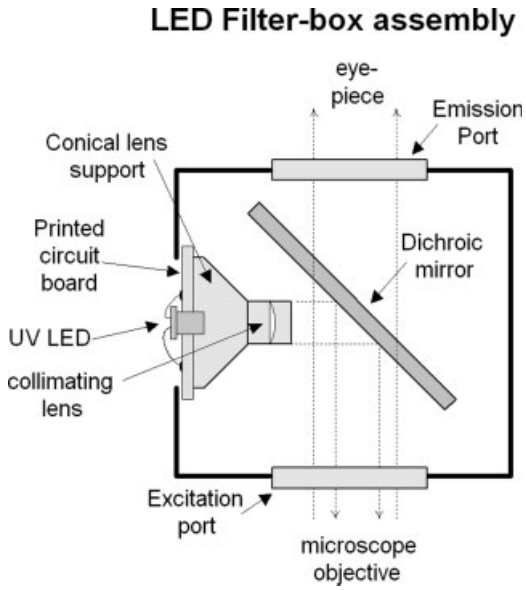

FIG. 2. The small size of the LED permitted the device to be mounted within the filter housing to simplify the optical arrangement. A single collimating lens was used to direct the LED output onto the dichroic filter that reflects UV whilst transmitting longer wavelengths (>400 nm). The fluorescent emission from the lanthanide chelate labeled target is spiked and centered at 617 nm and is transmitted effectively by the dichroic mirror.

Newton, NJ) was fixed about 5 mm from the LED face within a machined aluminium housing and adjusted to collimate LED emission. No attempt was made to achieve Koehler illumination in the prototype. The FT395 dichroic mirror strongly reflects UV wavelengths (<400 nm) but transmits longer wavelengths (>420 nm) and provides sufficient wavelength selection to permit removal of both the excitation and emission filters. The increased optical clarity helped maximize fluorescence collection and excitation efficiency of the instrument. The UV LED drive circuit (Fig. 3) is a simple design that employs a dual monostable multivibrator with a negative going input trigger. The second monostable is triggered by the rising edge of the collector voltage on the output transistor (Q11) and this ensures the LED is off when the camera trigger pulse is activated. The LED output drive transistor is a 2SC2335 with a rated fall-time of 1 μs and a storage time of 2.5 μs. These characteristics led to rounding of the falling edge (see Fig. 4), although the pulse was roughly square wave in shape with a duration of 101 μs. Image acquisition was done at a pulse frequency of 800 Hz using an external TTL pulse generator to drive the monostable circuit shown in Figure 3. For calibration purposes, the LED was operated using a direct current input of 500 mA and output power of the LED at 365 nm was measured using a Coherent FieldMax TO laser power meter.

Spectral measurements were made using an Ocean Optics spectrometer model USB2000 calibrated for the range 280–850 nm (Ocean Optics, Dunedin, FL). The USB2000 used for this work had been enhanced for operation in the UV through application (by the manufacturer) of a phosphor on the linear CCD detection element. The instrument was configured to capture spectral information following a hardware trigger (nanosecond resolution), and in this mode the instrument has a fixed 50-ms integration period. Hardware triggering was used to analyze the faint luminescence emanating from the LED following switch-off. To minimize transfer losses, the LED was fixed directly to the input slit of the spectrometer. The USB2000 spectrometer was also operated in conventional untriggered mode to observe both filtered (longpass >400 nm; FT395, Carl Zeiss, Australia) and unfiltered LED emission to gauge the relative intensities of the visible and UV components. The USB2000 spectrometer could accept a large range in signal intensity through adjustments to the spectrometer integration period. A silicon-photodiode was used to record the optical profile of the LED excitation pulse.

The time-gated image-intensified camera from the TGLM provided a means of verifying the decay lifetimes reported by the hardware-gated USB2000 spectrometer. The LED was mounted on the sample platform of the TGLM so that an image of the LED die could be captured at precise intervals following the falling edge of the excitation pulse. The

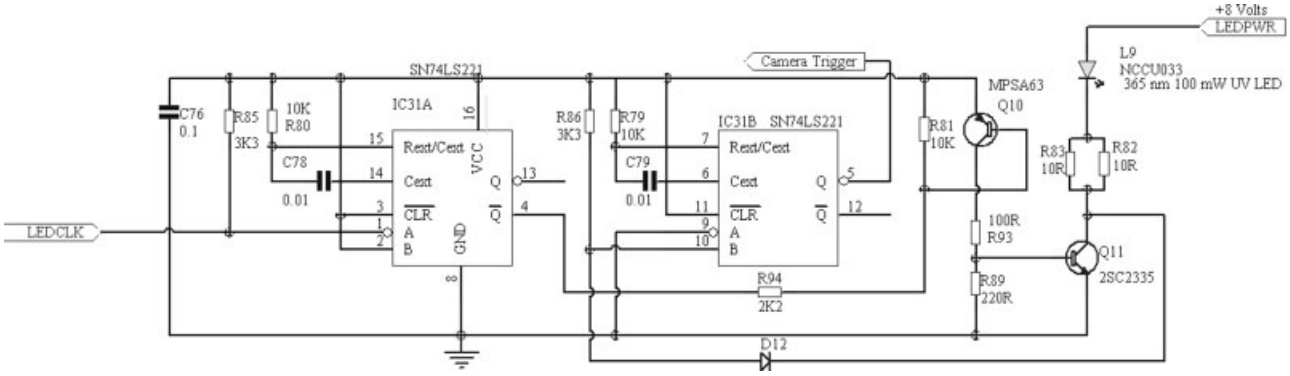

FIG. 3. Schematic diagram of the circuit used to drive the NCCU033 UV LED. The LEDCLK input is a standard TTL input and can be conveniently triggered from any TTL clock source at a frequency up to about 1 kHz. The camera trigger output is used to initiate the gate hold-off time period within the DicamPro camera and is delayed until the power transistor 2SC2335 has fully turned off as determined by diode D12.

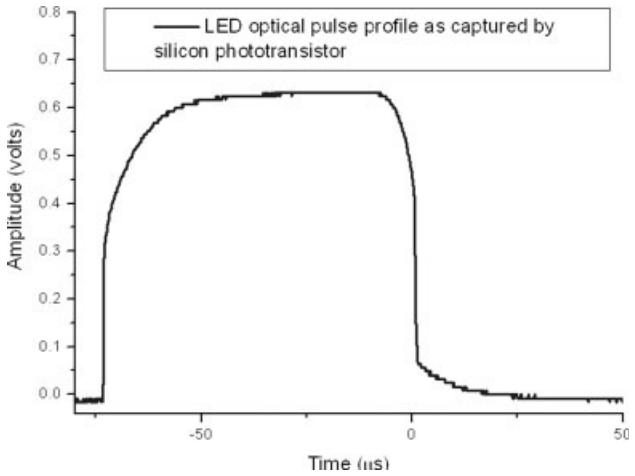

FIG. 4. Profile of the LED excitation pulse was measured with a silicon photodiode; pulse width was 101 µs in duration and the trailing edge response was extended primarily because of storage effects in the switching transistor and, to a smaller extent, by visible luminescence emitted by the LED following switch-off.

average pixel intensity for a segment of the LED die was recorded with and without a UV bandpass filter (U-340, EO Edmund, Singapore). The filter suppressed the relatively long-lived visible luminescence to permit measurement of the decay rate of the 360-nm emission. Electrical waveforms were captured on a 200-MHz, four-channel digital oscilloscope (TDS2024; Tektronix, Portland, OR).

Giardia cysts (Biotech Frontiers Pty, Sydney, Australia) were labeled using the europium chelate BHHST ((4,4′-bis-(1″,1″,1″,2″,2″,3″,3″-heptafluoro-4″,6″-hexanedion-6″-yl) sulfonyl-aminopropyl-ester-*N*-succinimide-ester-*o*-terphenyl)), the synthesis and use of which has previously been reported (11). The 10,000:1 concentrate of environmentally sourced water used for this work was a kind gift from Dr. Belinda Ferrari and was prepared from 10-L backwash water samples using the flocculation method (21).

Although porphyrin-based chelates, with their shorter fluorescence lifetimes, would perhaps have provided a more stringent test of the benefits of a LED-excited TGLM, we employed BHHCT/BHHST immunoconjugates instead due to their ready (in-house) availability and because we had gained some expertise in the preparation and use of these bioconjugates over a number of years. The autofluorescent water concentrate was spiked with *Giardia* cysts, filtered, and treated with a *Giardia* BHHST-immunoconjugate in situ (100 µL at 66 µg ml^{-1}; 15 min). The filter was then washed (3 × 500 µL H_2O) and vortexed in a 1.5-ml micro-reaction vial containing 300 µL of $NaHCO_3$ buffer (0.1 M, pH 8.5) and 0.6 mg ml^{-1} trioctylphosphine oxide (TOPO). A 2-µL aliquot of the suspension was transferred to a slide followed by 2 µL of a 0.0227 M $EuCl_3$ solution containing 200 mg ml^{-1} polyvinyl alcohol to thicken it to a syrup. The viscous solution slows movement and prevents motion blur during the image capture.

Origin 6.0 (Microcal Software, Northampton, MA) was used to format the data plots and calculate the standard deviation of the mean (standard error).

RESULTS

Luminous output of the UV LED at a distance 2 cm from the LED face was 30 mW cm^{-2} and this was reduced to 27.2 mW cm^{-2} after passage through the collimating lens. Power exiting from the filter cube (following reflection from the dichroic) was measured at 14.1 mW cm^{-2}, thus only about half the output from the LED was actually directed into the microscope objective. Filter-cubes from two different manufacturers were equipped with UV LEDs and both assemblies produced similar optical outputs (highest values shown here). The NCCU033 devices used in this work were engineering samples with lower directivity compared to current production. Relative power output was reduced 50% at 60° off-axis for the engineering samples compared to 45° for the production devices with better directivity. Although rated output of the devices at 500 mA was 100 mW cm^{-2}, only a portion of the output was captured by the optical sensor that was situated about 2 cm from the emitting face of the LED.

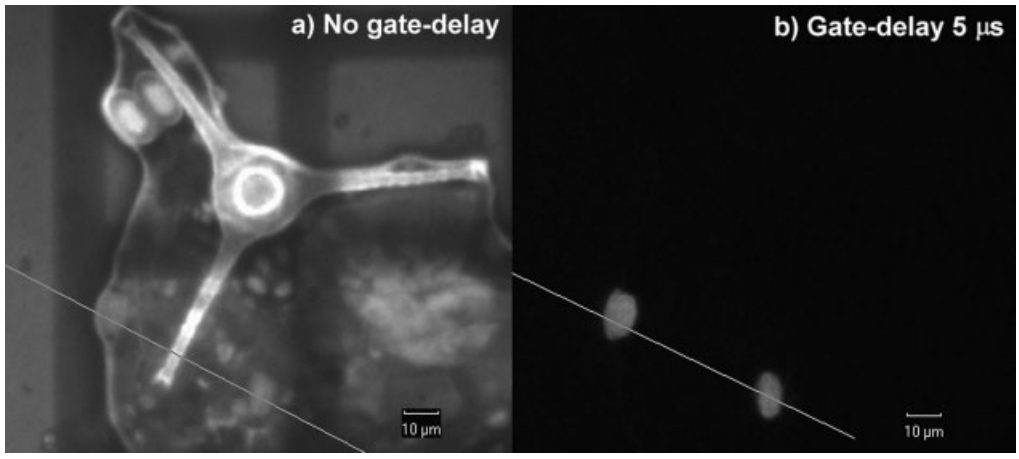

FIG. 5. (**a**) Two immunofluorescently labeled *Giardia* cysts embedded in an autofluorescent matrix of algae (line transects cysts) viewed with conventional epifluorescence and (**b**) using TGLM with UV-LED excitation.

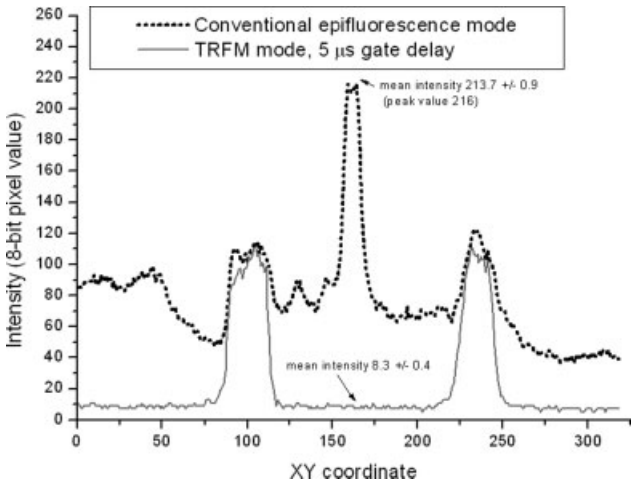

FIG. 6. Line profile transecting the two cysts shown in Figures 5a and 5b illustrates the large increase in SNR achieved with the LED-excited TGLM. Autofluorescence of the central peak (8-bit value of 213 ± 0.9) was reduced to background levels (average 8.3 ± 0.4) after a gate-delay of 5 μs.

In Figure 5a, the fluorescence of the central desmid (*Chlorophyta staurastrum*; the trigonal organism) is strong by comparison with the immunofluorescently labelled *Giardia* cysts when viewed in conventional epifluorescence mode. Autofluorescence is greatly suppressed, however, when a short gate-delay of 5 μs is imposed; the two *Giardia* cysts in the second frame are captured in stark relief against a dark background (Fig. 5b). The improvement in the signal-to-noise ratio (SNR) was determined by measuring the ratio of the fluorescent intensity of the cyst against (peak) autofluorescence intensity (pixel value on an 8-bit scale from 0 to 255) in conventional epifluorescence mode and in TGLM mode. The ratio of signal intensity to autofluorescence in conventional epifluorescence mode was 110.1 ± 1.3/213.7 ± 0.9, resulting in a SNR of 0.51 ± 0.013. A greatly improved SNR of 12.8 ± 0.76 was achieved using time-resolved mode (106.4 ± 1.2/8.3 ± 0.4) so that the effective improvement in SNR was ~25-fold (12.8/0.51). The images shown in Figures 5a and 5b were sampled as indicated by the white line to produce a line profile of intensity (see Fig. 6) that illustrates with improved clarity the reduction in autofluorescence that is achieved in TGLM mode. The SNR was calculated using the data reported from the line profile shown in Figure 6, however, if the peak intensity of the autofluorescence (measured at the desmid central ring; 252) is substituted into the equation, the improvement in the achieved SNR was nearly 30-fold. The large enhancement in SNR was typical for all frames captured in TRL mode in which labeled cysts were present. A key advantage of the LED excitation over flashlamp-based systems is the absence of any significant luminous output shortly after the excitation pulse is extinguished (>5 μs). BHHST chelate has a typical fluorescence lifetime (τ) of between 240 and 620 μs (depending on buffer solution) and is diminished by ~2% in the first instance and 0.8% in the second instance when a gate-delay of 5 μs is imposed. A significantly greater loss of fluorescence intensity occurs when the emission is captured after a gate-delay of 50 μs with losses of 18.8% and 7.7% respectively. The longer gate-delay is required for a flashlamp TGLM to permit decay of flashlamp plasma. Light from the flashlamp plasma is still present at significant levels for up to 100 μs following the main arc discharge and this causes further degradation of the SNR. Thus SNR is optimized in a LED-excited system by ensuring the gate hold-off time period is just sufficient to ensure zero excitation energy is present.

Characteristics of the LED Excitation Source

UV emission from the LED is strongly spiked with a FWHM of 10 nm (362–372 nm), as shown in Figure 7a. The amplitude of the visible emission during normal

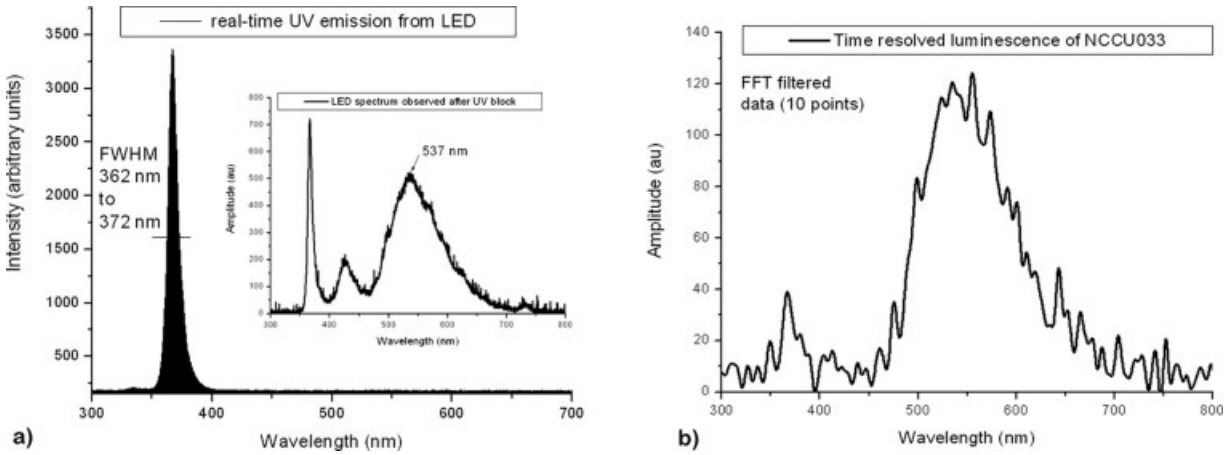

FIG. 7. (**a**) The real-time LED emission spectrum is centered at 364.5 nm with a FWHM spanning 362–372 nm. The inset shows the visible portion of the spectra that is more than three orders of magnitude less intense than the peak at 365 nm. (**b**) is a plot of time-gated emission from the LED captured shortly after current injection had ceased. Emission at 366 nm was barely discernible because of the very rapid decay lifetime for this component. The plot was smoothed with a low-pass filter to eliminate noise spikes using the fast Fourier transform (FFT) option (10 samples) within Origin 7.0.

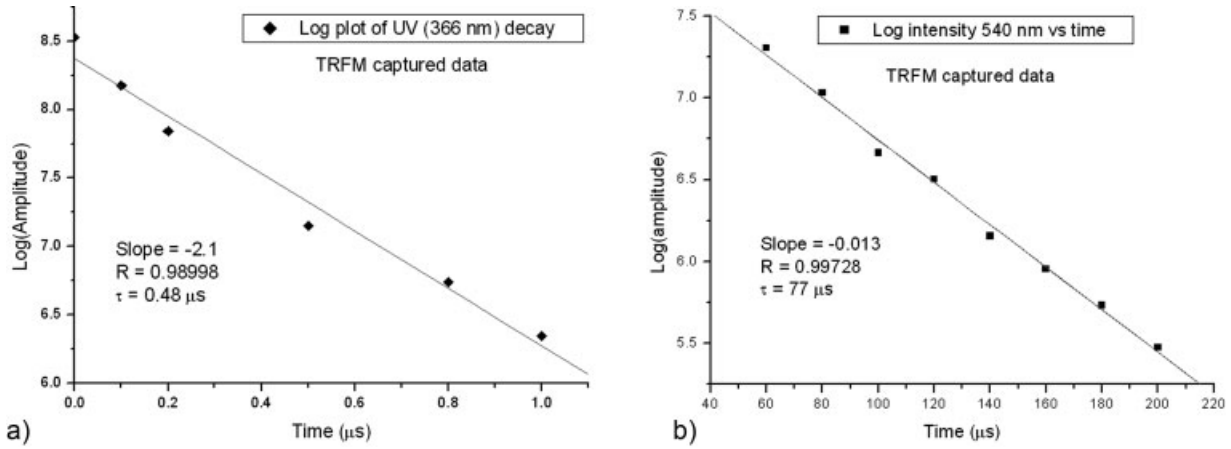

FIG. 8. Both the UV and visible components of the luminescence spectra decay with complex decay kinetics. (**a**) is a logarithmic plot of 366 nm intensity vs. time after current injection into the LED had ceased. Although the decay is multi-exponential in nature, it may be approximated portion-wise using single exponential kinetics. The negative reciprocal of the slope provides an estimate of the single exponential decay lifetime constant of 480 ± 34 ns and (**b**) similarly is a log plot of amplitude at 540 nm vs. time for the period 40–200 μs. Visible emission decays rapidly within the first 40 μs with an approximate (single exponential) lifetime of 40 μs. Subsequently, the decay kinetics follow near single exponential kinetics ($R = 0.99728$) with a decay lifetime of 77.2 ± 2.3 μs.

operation of the LED is very low by comparison with the 366-nm component, and blocking of the UV was necessary to estimate visible intensity. The inset in Figure 7a illustrates the spectrum recorded by the USB2000 spectrometer after insertion of a UV stop-filter. LED intensity at 366 nm was 3,930 (au) with an integration period of 3 ms and this was reduced 5.44-fold when a UV stop-filter (FT-395) was introduced into the beam path (integration period of 1 s). The correction factor for the difference in integration periods was 333, and after adjusting for filter insertion losses (data not shown), the actual signal intensity at 537 nm was 626/333, or 1.88. Thus peak intensity at 366 nm was 3,930/1.88 or 2,090-fold that at 537 nm. Luminescence from the LED was captured using hardware gating of the USB2000 and the decay lifetime for the 537-nm component was estimated to be 81.8 ± 4.3 μs, whereas a more accurate figure of 77.2 ± 2.3 μs was determined using the TGLM. As noted in Materials and Methods, the USB2000 used for this work was enhanced for operation in the UV through application of a phosphor on the linear CCD detection element. Luminescence of this phosphor introduced large errors when attempting to measure the decay rate of UV LED emission, and the time-gated CCD camera on the TGLM was relied upon to determine this parameter. Experimental work performed with a mechanical chopper wheel (rise time of 15 μs) had proven inadequate to measure the rapid decay rate of the UV component, yet supported the data obtained from the TGLM that is shown as a logarithmic plot of amplitude versus time in Figure 8a. The UV emission decay kinetics could be approximated with reasonably good fit ($R = 0.98998$) using single-exponential decay kinetics and a lifetime of 480 ± 34 ns. The integrated luminous output of a single band-pass filtered UV pulse 101 μs in duration was compared to the residual UV emission and determined to be 584-fold greater (data not shown). Lifetime of the visible luminescence (Fig. 8b) was also estimated using the single-exponential decay model and a logarithmic plot of intensity vs. time for the period 40–200 μs yielded a slope of −0.01296, equivalent to a lifetime of 77.2 ± 2.3 μs. Visible luminescence was observed to increase rapidly as current injection was increased to about 100 mA, thereafter reaching a plateau whilst UV emission continued to rise linearly with current. At low injection current (100 mA), peak amplitude of the visible emission was recorded at 537 nm and at the moment of switch-off, was 1:2,090 that of 366 nm intensity. When a more typical injection current of 600 mA was used, the ratio of peak amplitudes was 1:11,426 and the ratio of integrated emission 1:1,433 (data not shown).

DISCUSSION

Spectral selection techniques achieve probe discrimination by careful choice of fluorophore and the use of appropriate excitation/emission filter sets. This is a useful strategy when autofluorescence is confined to particular regions of the spectrum and suitable probe fluorophores are available for the more sparsely occupied spectral regions. The "water-concentrate" obtained from the Sydney water supplies using flocculation was richly autofluorescent and contained numerous species of algae and desmids together with plant and mineral debris. The relative merits of spectral techniques versus TRF methods for water-concentrate samples has been reported earlier (20) and only TRF techniques are discussed in the work reported here. The large improvement in SNR achieved with LED-excited TGLM would be reduced marginally, had the final (TRL) image been compared with that obtained using a conventional epifluorescence microscope equipped with the appropriate filter combination. Nevertheless, our experience has shown that using conventional fluorescence microscopy, no filter-set combination was adequate to permit the ready detection of immunofluorescently labeled *Giardia* or *Cryptosporidium* within the autoflu-

orescent matrix of water-concentrates without prior enrichment.

The long fluorescence lifetime of lanthanide chelate probes is a valuable discriminating parameter to isolate probe fluorescence from nonspecific background autofluorescence. The use of time-resolved luminescence techniques has been hindered somewhat by the relatively low fluorescence yields obtained using these systems. The problem has been attacked both from the viewpoint of increasing fluorescence yield through use of more efficient high-yielding fluorophores (such as BHHST) and through improvements in instrumentation. Pulse fluorometry based methods rely on capturing the probe fluorescence shortly after the excitation phase has ceased and autofluorescence has faded. Flashlamps require the period following the primary excitation pulse to be extended far longer than that required for autofluorescence decay. This is necessary to allow the glowing flashlamp plasma to fade to an acceptably low level that typically takes more than 50 μs (15,20). As a consequence of this relatively long gate-delay, only fluorophores with lifetimes of hundreds of microseconds are suitable as probes for flashlamp-excited time-resolved luminescence. Porphyrin-based chelates of palladium and platinum have been reported to be intensely fluorescent, yet their short fluorescence lifetimes (<100 μs) are a critical limiting parameter with flashlamp-based instruments.

UV LEDs have only recently become available at wavelengths suitable for exciting fluorescence from BHHST (optimum λ = 337 nm). The wavelength of 365 nm is about 40% effective as 337 nm, whereas 375 nm is about 14% as effective as 337 nm. The unprecedented power available from these devices is a key factor in determining their great utility. Driven moderately hard in pulse-mode, these UV LEDs were found capable of delivering twice their rated output (data not shown) and radiate sufficient UV energy to bleach europium chelate polymer beads (Fluorospheres F2088-2; Molecular Probes, Invitrogen Australia P/L, Mt. Waverly, VIC, Australia) within less than a minute. These beads had previously been noted to resist photobleaching when excited using moderate intensity illumination from Hg-vapor lamps.

The second factor of great importance relates to the electrical characteristic of LED that enables very rapid switching of these devices. Typically LEDs can be switched within a couple of nanoseconds, however, as a consequence of trapped states within the gallium nitride lattice (22,23), some residual long-lived emission is observed in the visible for the UV LEDs. The broad visible luminescence represents unwanted optical output from the excitation source and must be removed to ensure that the key advantage of time-resolved techniques, low background, is maintained. This is not considered a serious limitation for TGLM, since visible emission integrated over the entire band was three orders of magnitude (1,433-fold) less than UV emission at the moment of switch-off. The dichroic mirror (FT395) used in the filter-cube strongly reflects UV but transmits more than 90% of wavelengths from 410 to 750 nm, and thus very little visible luminescence reaches the image sensor.

Fortunately the UV component decays very rapidly following switch-off with an observed lifetime of 0.48 μs, and after 5 μs this component is present at 3×10^{-5} its initial intensity.

Another significant advantage of LED excitation was the high repetition rate that permitted acquisition times to be reduced from 8 s with the xenon flashlamp to less than half a second with the LED. Background levels were reduced by half with LED excitation when compared with images acquired using the xenon flashlamp (8.4 vs. 17) (20). This is a consequence of three factors: the rapid (UV) falling edge of the LED ensures that the excitation and fluorescence emission phases are separate and discrete events in the TGLM, thus permitting the removal of the emission filter to improve optical clarity and increase collection efficiency at the image intensifier. Secondly, the rapid LED switch-off permits the gate-delay to be reduced from 50 to 5 μs so as to harvest fluorescence emission at its peak, an improvement of 20% in captured light quanta. Thirdly, plasma generated in the xenon flashlamp persists for many hundreds of microseconds and still registers on the image intensifier after the hold-off time of 50 μs, subtly adding to background and decreasing SNR.

Another significant advantage arises from mounting the LED directly in the filter-cube, since this configuration eliminates the need for beam guiding optics (with the associated losses), thereby increasing excitation efficiency. High-power LEDs operating at 365 nm were found to be near ideal excitation source for TGLM applications employing lanthanide chelates.

LITERATURE CITED

1. Blom H, Johansson M, Hedman A-S, Lundberg L, Hanning A, Hard S, Rigler R. Parallel fluorescence detection of single biomolecules in microarrays by a diffractive-optical-designed 2 × 2 fan-out element. Appl Opt 2002;41:3336–3342.
2. Rost FWD. Fluorescence Microscopy. Cambridge: Press Syndicate of the University of Cambridge; 1995. 457 pp.
3. Connally R, Veal D, Piper J. High resolution detection of fluorescently labeled microorganisms in environmental samples using time-resolved fluorescence microscopy. FEMS Microbiol Ecol 2002;41:239–245.
4. Lakowicz JR. Principles of Fluorescence Spectroscopy, 2nd ed. New York: Plenum; 1999. 496 pp.
5. Gaviola E. Ein Fluorometer. Apparat zur Messung von Fluoreszenzabklingungszeiten. Z Phys 1927;42:853–861.
6. Takalo H, Mukkala VM (to Wallac Oy, Finland). Luminescent lanthanide chelates for immunoassays and other uses, and their preparation. WO Patent 9,311,433. 1993.
7. Seveus L, Vaisala M, Syrjanen S, Sandberg M, Kuusisto A, Harju R, Salo J, Hemmila I, Kojola H, Soini E. Time-resolved fluorescence imaging of Europium chelate label in immunohistochemistry and *in-situ* hybridization. Cytometry 1992;13:329–338.
8. Soini EJ, Pelliniemi LJ, Hemmila IA, Mukkala VM, Kankare JJ, Frojdman K. Lanthanide chelates as new fluorochrome labels for cytochemistry. J Histochem Cytochem 1988;36:1449–1451.
9. Xiao M, Selvin PR. Quantum yields of luminescent Lanthanide chelates and Far-red dyes measured by resonance energy transfer. J Am Chem Soc 2001;123:7067–7073.
10. Soini AE, Kuusisto A, Meltola NJ, Soini E, Seveus L. A new technique for multiparameter imaging microscopy: Use of long decay time photoluminescent labels enables multiple color immunocytochemistry with low channel-to-channel crosstalk. Microsc Res Tech 2003;62:396–407.
11. Connally RE, Veal DA, Piper J. Time-resolved fluorescence microscopy using an improved europium chelate BHHST for the in-situ detection of Cryptosporidium and Giardia. Microsc Res Tech 2004;64:312–322.
12. Li M, Selvin PR. Luminescent Polyaminocarboxylate chelates of Terbium and Europium: The effect of chelate structure. J Am Chem Soc 1995;117:8132–8138.

13. Hemmila I, Mukkala VM, Latva M, Kiilholma P. Di- and Tetracarboxylate derivatives of pyridines, bipyridines and terpyridines as luminogenic reagents for time-resolved fluorometric determination of Terbium and Dysprosium. J Biochem Biophys Methods 1993;26:283–290.
14. Kaeberlein T, Lewis K, Epstein SS. Isolating "Uncultivable" microorganisms in pure culture in a simulated natural environment. Science 2002;296:1127–1129.
15. Vereb G, Jares-Erijman E, Selvin PR, Jovin MT. Temporally and spectrally resolved imaging microscopy of lanthanide chelates. Biophys J 1998;74:2210–2222.
16. Zotikov AA, Polyakov YS. The use of the phosphorescence microscope for the study of the phosphorescence of various cells. Microsc Acta 1977;79:415–418.
17. Sutherland JC, Cimino GD, Desmond EJ. Simultaneous measurement of fluorescence and phosphorescence using synchronously gated photon counters. Anal Biochem 1979;97:158–165.
18. Latva MHT, Mukkala V-M, Matachescu C, Rodriguez-Ubis JC, Kankar J. Correlation between the lowest triplet state energy level of the ligand and lanthanide(III) luminescence quantum yield. J Lumin 1997;75: 149–169.
19. Hennink RJ, de Haas R, Verwoerd NP, Tanke HJ. Evaluation of a time-resolved fluorescence microscope using a phosphorescent Pt-porphine model system. Cytometry 1996;24:312–320.
20. Connally R, Veal D, Piper J. Flashlamp excited time-resolved fluorescence microscope suppresses autofluorescence in water concentrates to deliver 11-fold increase in signal to noise ratio. J Biomed Opt 2004;9:725–734.
21. Vesey G, Slade JS, Byrne M, Shepherd K, Fricker CR. A new method for the concentration of *Cryptosporidium* oocysts from water. J Appl Bacteriol 1993;75:82–86.
22. Reshchikov MA, Morkoc H. Luminescence properties of defects in GaN. J Appl Phys 2005;97:061301/1–061301/95.
23. Seager CH, Tallant DR, Yu J, Gotz W. Luminescence in GaN co-doped with carbon and silicon. J Lumin 2004;106:115–124.